JOC Article

Enantiomerization of Chiral Uranyl−Salophen Complexes via Unprecedented Ligand Hemilability: Toward Configurationally Stable Derivatives

Alessia Ciogli,[†] Antonella Dalla Cort,*[,‡] Francesco Gasparrini,*[,†] Lodovico Lunazzi,[§] Luigi Mandolini,[‡] Andrea Mazzanti,[§] Chiara Pasquini,[‡] Marco Pierini,[†] Luca Schiaffino,[‡] and Francesco Yafteh Mihan[‡]

Dipartimento di Chimica and IMC-CNR Sezione Meccanismi di Reazione, Università La Sapienza, Box 34 Roma 62, 00185 Roma, Italy, Dipartimento di Studi di Chimica e Tecnologia delle Sostanze Biologicamente Attive, Università La Sapienza, Piazzale Aldo Moro 5, 00185 Roma, Italy, and Dipartimento di Chimica Organica "A Mangini", Università di Bologna, Viale Risorgimento 4, 40136 Bologna

antonella.dallacort@uniroma1.it; francesco.gasparrini@uniroma1.it

Received March 28, 2008

In the search for configurationally stable inherently chiral uranyl−salophen complexes, the newly synthesized compound **3** featuring a dodecamethylene chain was expected to be a promising candidate. Unexpectedly, dynamic HPLC on a enantioselective column showed that it still undergoes enantiomerization at high temperature. By comparison with the dynamic behavior of compounds **4** and **5**, it was found that the enantiomerization rate is independent of the size of the ligand. This finding definitely rules out a jump rope-type mechanism for the enantiomerization process and points to reaction pathways involving preliminary rupture of one of the O···U coordinative bonds. This provides unprecedented evidence of the occurrence of ligand hemilability in metal−sal(oph)en complexes. Such findings inspired the synthesis of compound **6** endowed with a more rigid spacer, i.e., that derived from 4,4′-(1,4-phenylenediisopropylidene)bisphenol. DHPLC investigations showed that the new structural motif imparts a higher configurational stability, thus raising the half-life for the enantiomerization to more than 2 months at room temperature. This clearly establishes that this compound represents the first member of a new class of inherently chiral receptors, whose potential in chiral recognition and catalysis now can be feasibly explored.

Introduction

A major motivation for the continuing interest in the design and synthesis of novel chiral receptors arises from their potential applications in the fields of enantioselective recognition[1] and asymmetric catalysis.[2] A variety of structural motifs have been used so far in the design of such kinds of systems and among

* Corresponding author. Phone: +39 06 49913087 (A.D.C.), +39 06 49912776 (F.G.). Fax: +39 06 490421 (A.D.C.), +39 06 49912780 (F.G.).
[†] Dipartimento di Studi di Chimica e Tecnologia delle Sostanze Biologicamente Attive, Università La Sapienza.
[‡] Dipartimento di Chimica and IMC-CNR Sezione Meccanismi di Reazione, Università La Sapienza.
[§] Università di Bologna.

(1) (a) Stibor, I.; Zlatuskova, P. Chiral Recognition of Anions. In *Anion Sensing*; Stibor, I., Ed.; Topics in Current Chemistry 255;Springer: Berlin, Germany, 2005; pp 31−63. (b) Heo, J.; Mirkin, C. A. *Angew. Chem., Int. Ed.* **2006**, *45*, 941–944. (c) Ikeda, T.; Hirata, O.; Takeuchi, M.; Shinkai, S. *J. Am. Chem. Soc.* **2006**, *128*, 16008–16009. (d) Miyaji, H.; Hong, S.-J.; Jeong, S.-D.; Yoon, D.-W.; Na, H.-K.; Hong, J.; Ham, S.; Sessler, J. L.; Lee, C.-H. *Angew. Chem., Int. Ed.* **2007**, *46*, 2508–2511. (e) Yakovenko, A. V.; Boyko, V. I.; Kalchenko, V. I.; Baldini, L.; Casnati, A.; Sansone, F.; Ungaro, R. J. *Org. Chem.* **2007**, *72*, 3223–3231.

10.1021/jo800610f CCC: $40.75
Published on Web 07/16/2008

them those based on metal complexes with vacant coordination sites appear quite appealing.[3]

Complexes of *N*,*N*′-phenylene−salicylidene (salophen) ligands with the uranyl dication[4] have been widely employed as receptors for anions and neutral molecules in organic solvents,[5] and as supramolecular catalysts[6] of reactions that undergo electrophilic metallocatalysis. It can be expected that once made chiral these complexes would be of interest as enantioselective receptors and catalysts. The UO_2^{2+} cation has a well-known preference for pentagonal bipyramidal coordination with the two oxygen atoms in the apical positions and the N_2O_2 donor atoms of the salophen ligand in four of the five equatorial coordination sites.[7] Hence the fifth position is available for labile coordination to a monodentate ligand (G), as shown in **1**. This feature makes uranyl−salophen complexes suitable for the design of supramolecular hosts because the location of the bound guest can be clearly predicted and a structured binding site is easily shaped by the introduction of proper substituents in one or in both ortho positions with respect to the phenoxide oxygen atoms.

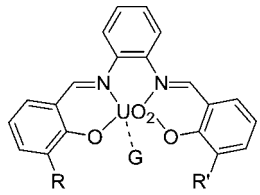

1

Another peculiarity of these derivatives is that, upon complexation, the salophen ligand is forced to assume a nonplanar U-shaped geometry to accommodate the large uranium atom. The direct consequence is that compounds such as **1** belong to the C_s or C_1 symmetry group depending on whether the substituents R and R′ are identical or not. This means that nonsymmetrically substituted derivatives are chiral[8] and might find use in the field of enantioselective recognition and asymmetric catalysis. Clearly the great interest toward such inherently chiral[9] derivatives is that the presence of the three interacting sites (i.e., the metal center and the groups R and R′)

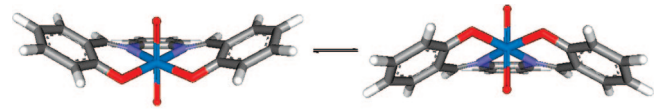

FIGURE 1. Flipping motion in uranyl−salophen complex **1** (R = R′ = H).

allows the build up of an easily predictable chiral spatial array without limiting the choice of starting materials to chiral synthons.

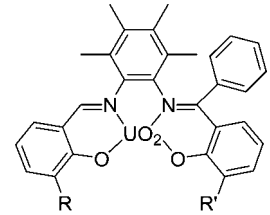

2

Unfortunately the finding that the two enantiomers are in fast equilibrium through a flipping motion that inverts the ligand curvature[8] (Figure 1) has precluded so far the use of uranyl−salophen complexes in chiral recognition and catalysis. This motion can be slowed down by bulky substituents in the imine bonds region as in compounds **2** whose enantiomerization half-life is about 17 h at 25 °C ($\Delta G^{\#} = 24.6$ kcal mol^{-1}),[10] but this leads to an increase in the ligand curvature that reduces the strength of the association between the metal and the ligand and ends up in two major drawbacks. First, resolution via chiral HPLC, as well as standard chromatographic purifications, are precluded because upon these treatments such severely distorted complexes dissociate to give the free ligand. Second, the half-life reported above appears to closely approach a higher limit, since any further increase in steric bulk destabilizes the corresponding complexes to such an extent that they do not form at all. Alternatively, the configurational stability can be increased, without perturbing the strength of the association, by connecting the 5,5′ positions of the side rings with a spacer of proper length. Obviously the spacer should not be too short to induce high strain energy in the macrocyclic derivative, neither too long to enable curvature inversion through conformational motions of the jump-rope type. Such requirements are fulfilled by a 12-methylene chain, as shown by the fact that a complex with this structural motif survived to HPLC treatment and its enantiomers could be separated on a chiral stationary phase at room temperature.[11]

In the present paper we report on the synthesis of a new chiral macrocyclic uranyl−salophen derivative **3** and on a study of its configurational stability carried out by dynamic chiral HPLC. Quite surprisingly, this compound still undergoes enantiomerization at 80 °C on the time scale of the HPLC experiments. This rather unexpected result, together with those obtained for the newly synthesized complexes **4** and **5**, shed light on the mechanism of enantiomerization and provided unprecedented evidence for the occurrence of a ligand hemilability phenomenon in metal−sal(oph)en complexes. Such findings inspired the

(2) (a) Jacobsen, E. N.; Pfaltz, A. *Catalysis*; Springer: Berlin, Germany, 1999. (b) Matsumoto, K.; Saito, B.; Katsuki, T. *Chem. Commun.* **2007**, 3619–3627. (c) *New Frontiers in Asymmetric Catalysis*; Mikami, K., Lautens, M., Eds.; John Wiley & Sons: Hoboken, NJ 2007, and references cited therein.

(3) (a) Rogers, C. W.; Wolf, M. O. *Coord. Chem. Rev.* **2002**, *233*−*234*, 341–350. (b) Beer, P. D.; Bayly, S. R. Anion sensing by metal-based receptors. In *Anion Sensing*; Stibor, I., Ed.; Topics in Current Chemistry 255;Springer: Berlin, Germany, 2005; pp 125−162.

(4) (a) Pfeiffer, P.; Hesse, T.; Pfitzner, H.; Scholl, W.; Thielert, H. J. *Prakt. Chem.* **1937**, 217. (b) Bandoli, G.; Clemente, D. A.; Croatto, U.; Vidali, M.; Vigato, P. A. *J. Chem. Soc., Chem. Commun.* **1971**, 1330–1331.

(5) (a) Antonisse, M. M. G.; Reinhoudt, D. N. *Chem. Commun.* **1998**, 443–448. (b) van Axel Castelli, V.; Dalla Cort, A.; Mandolini, L.; Pinto, V.; Reinhoudt, D. N.; Ribaudo, F.; Sanna, C.; Schiaffino, L.; Snellink-Ruël, B. H. M. *Supramol. Chem.* **2002**, *14*, 211–219. (c) Dalla Cort, A.; Pasquini, C.; Miranda Murua, J. I.; Pons, M.; Schiaffino, L. *Chem. Eur. J.* **2004**, *10*, 3301–3307. (d) Cametti, M.; Nissinen, M.; Dalla Cort, A.; Mandolini, L.; Rissanen, K. *J. Am. Chem. Soc.* **2007**, *129*, 3641–3648.

(6) (a) van Axel Castelli, V.; Dalla Cort, A.; Mandolini, L.; Reinhoudt, D. N. *J. Am. Chem. Soc.* **1998**, *120*, 12688–12689. (b) van Axel Castelli, V.; Dalla Cort, A.; Mandolini, L.; Reinhoudt, D. N.; Schiaffino, L. *Chem. Eur. J.* **2000**, *6*, 1193–1198. (c) van Axel Castelli, V.; Dalla Cort, A.; Mandolini, L.; Reinhoudt, D. N.; Schiaffino, L. *Eur. J. Org. Chem.* **2003**, *62*, 7–633. (d) Dalla Cort, A.; Mandolini, L.; Schiaffino, L. *Chem. Commun.* **2005**, 3867–3869. (e) van Axel Castelli, V.; Dalla Cort, A.; Mandolini, L.; Pinto, V.; Schiaffino, L. *J. Org. Chem.* **2007**, *72*, 5383–5386.

(7) (a) Sessler, J. L.; Melfi, P. J.; Pantos, G. D. *Coord. Chem. Rev.* **2006**, *250*, 816–843. (b) Ephritikhine, M. *Dalton Trans.* **2006**, 2501–2516. (c) Takao, K.; Ikeda, Y. *Inorg. Chem.* **2007**, *46*, 1550–1562.

(8) Dalla Cort, A.; Mandolini, L.; Palmieri, G.; Pasquini, C.; Schiaffino, L. *Chem. Commun.* **2003**, 2178–2179.

(9) Dalla Cort, A.; Mandolini, L.; Pasquini, C.; Schiaffino, L. *New J. Chem.* **2004**, *28*, 1198–1199.

(10) Dalla Cort, A.; Mandolini, L.; Pasquini, C.; Schiaffino, L. *Org. Lett.* **2004**, *6*, 1697–1700.

(11) Dalla Cort, A.; Mandolini, L.; Pasquini, C.; Schiaffino, L. *J. Org. Chem.* **2005**, *70*, 9814–9821.

SCHEME 1. Synthetic Procedure for Compounds 3−5[a]

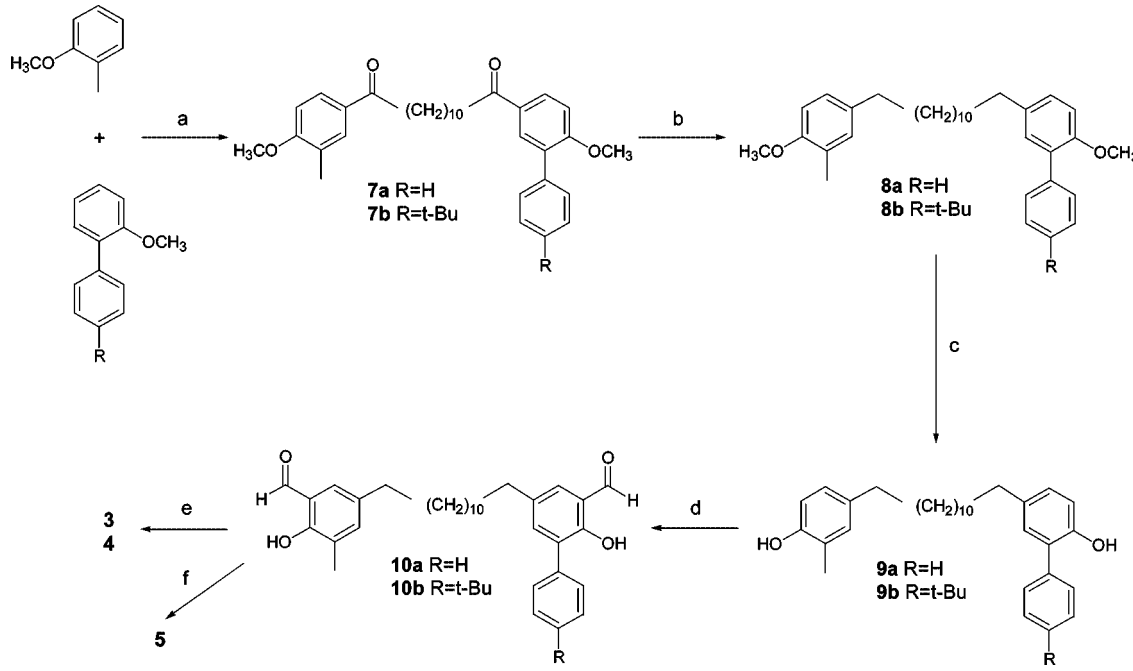

[a] Reagents and conditions: (a) $AlCl_3$, $ClCO(CH_2)_{10}COCl$; (b) $NaCNBH_3$, ZnI_2, $ClCH_2CH_2Cl$; (c) BBr_3, dry toluene; (d) $TiCl_4$, Cl_2CHOCH_3, dry CH_2Cl_2, 0 °C; (e) 1,2-diaminobenzene, $UO_2(OAc)_2 \cdot 2H_2O$, CH_3OH; (f) 1,2-diaminonaphthalene, $UO_2(OAc)_2 \cdot 2H_2O$, CH_3OH.

design and synthesis of compound **6**, whose enhanced configurational stability supports the proposed mechanism and offers prospect for the use of uranyl−salophen complexes as enantioselective receptors and catalysts.

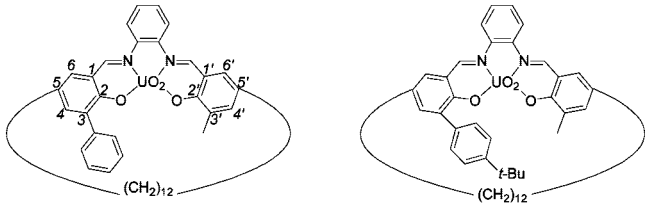

3 **4**

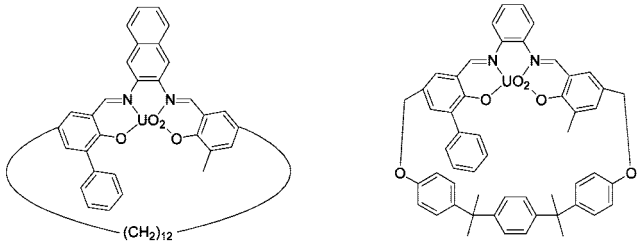

5 **6**

Results and Discussion

Macrocyclic complex **3** was prepared according to Scheme 1.[11] Its chirality was confirmed by the splitting of a number of ^{1}H NMR peaks caused by the addition of a 10-fold molar excess of *R*-(−)-2,2,2-trifluoro-1-(9-anthryl)ethanol in $CDCl_3$.[12] Analytical separations of the enantiomers were carried out at 40 °C with high enantioselectivity ($k_1' = 3.00$, $\alpha = 2.91$) on a cellulose-based Chiralcel-OD chiral stationary phase (CSP), using ternary mixtures of *n*-hexane/ethanol/$CHCl_3$ (50/30/20, v/v/v) as eluent (Figure 2). Chromatographic experiments at higher temperatures (Figure 3) unexpectedly revealed that this compound still undergoes enantiomerization at appreciable rates, as shown by the plateau region between the peaks of the separated enantiomers. Line shape analysis of the chromatograms gave numerical values of the first-order rate constants of enantiomerization, from which the enantiomerization barriers $\Delta G^{\#}$ were calculated (Table 1).

A dissociation−reassociation process in which the ligand releases the uranyl dication, undergoes free conformational changes, and eventually recombines with the metal was excluded because reassociation could hardly take place under chromatographic conditions. A simple jump rope-type mechanism, in which the polymethylene chain passes from one side to the other without dissociation−reassociation, seemed unlikely, but was not excluded a priori. Obviously, such a motion would be prevented by suitable extensions of the ligand structure. For that reason we synthesized cyclophanes **4** and **5** (Scheme 1), in which jump rope would be strongly hindered, depending on whether the chain swings from one side to the other over the aromatic pendant or over the 1,2-diaminobenzene moiety, respectively. However, when subjected to dynamic HPLC, both compounds **4** and **5** exhibited temperature-dependent chromatograms (Figures 2S and 3S in the Supporting Information) consistent with enantiomerization processes whose calculated barriers (Table 1) were almost indistinguishable from that of **3**. These findings, consistent with the rigidity revealed by the calculated structures of **3**−**5** (Figure 4), definitely ruled out the simple jump rope hypothesis for enantiomerization and posed an intriguing mechanistic challenge.

Ligand Hemilability: A Key to Understanding the Enantiomerization Mechanism. Ligand hemilability is a well-documented phenomenon occurring in transition metal com-

(12) Pirkle's method was used because no diastereotopic nuclei were available in the molecule.

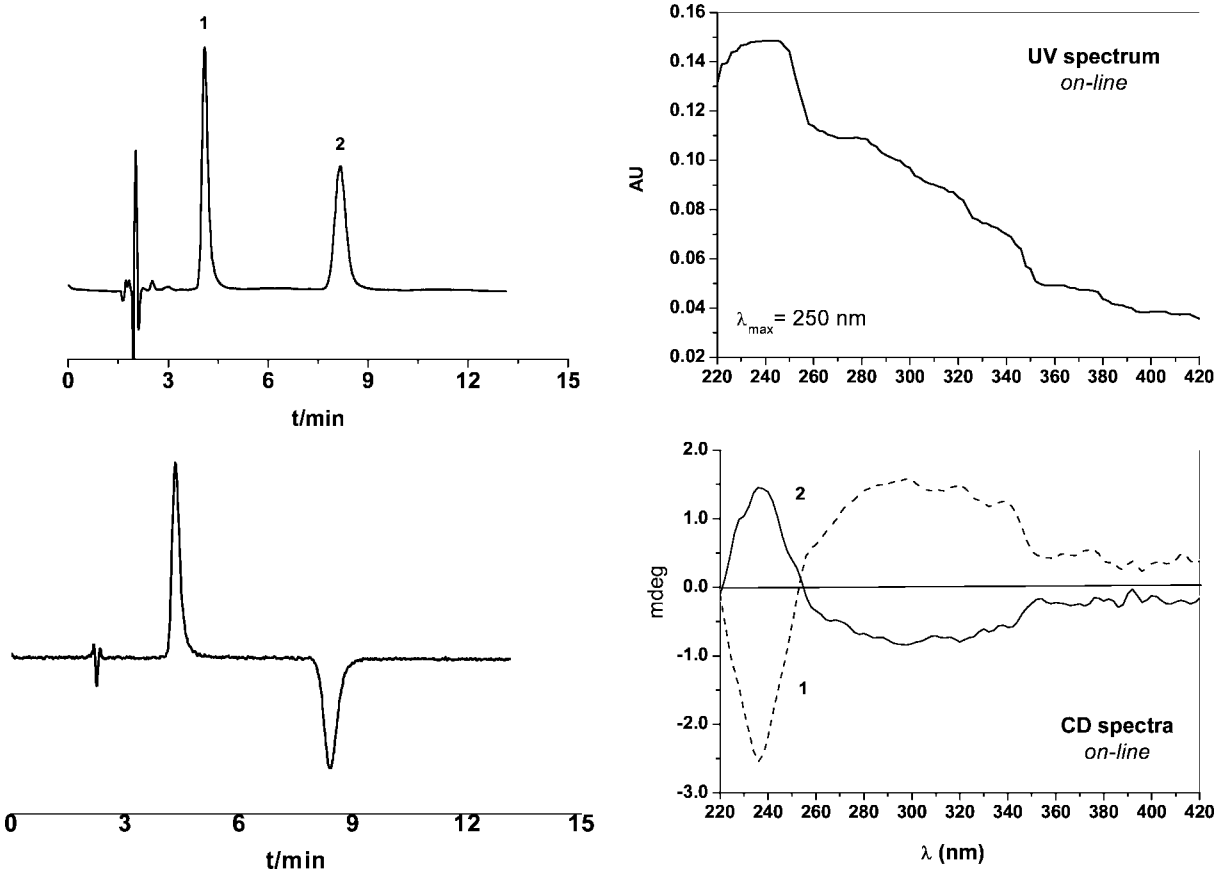

FIGURE 2. Analytical separation of the enantiomers of **3** by enantioselective HPLC at 40 °C. UV (top) and CD (bottom) chromatographic traces at 400 nm (left) and corresponding *online* spectra (right).

plexes of bidentate or multidentate hybrid ligands.[13] It can be defined as the property of such complexes to undergo a metal chelate opening process by rupture of one (usually the weakest) coordinative bond. Although unprecedented for Schiff base $N_2O_2^{2-}$ tetradentate ligands,[14] hemilability in complexes **3**−**5** offers a unique key to the intriguing problem of the enantiomerization mechanism. In its simplest version, a mechanistic hypothesis based on ligand hemilability involves rupture of the O···U bond on the side of the aromatic pendant. Subsequent 180° rotation around the single bond connecting the imine carbon atom and the phenoxide ring brings the two ends of the dodecamethylene chain closer to one another. The chain appears now to be long enough to pass over the methyl group, as depicted in Scheme 2, path A. A further 180° rotation, followed by recombination of the phenoxide with the uranium, would complete the enantiomerization process. The proposed mechanism is clearly consistent with the finding that identical barriers were measured for compounds **3**−**5**, because in the tricoordinated intermediate there is no steric interaction between the dodecamethylene chain and the aromatic pendant or the diamino-substituted ring. Rupture of one oxygen−metal bond, followed by 360° rotation of the phenoxide ring and its eventual recoordination, is clearly a silent process when occurring in complexes such as **1** (R = R′) or even in achiral symmetrically substituted macrocyclic derivatives. This explains why ligand hemilability, to the best of our knowledge, had never been reported before in metal−salen and −salophen complexes. It is the chirality of complexes **3**−**5**, coupled with their relatively high configurational stability, that removes the degeneracy and allows an otherwise silent process to be detected.

To obtain further insight into the conformational behavior of compound **3** under the hypothesis that a hemilability process does actually take place, some calculations based on molecular dynamics simulations were performed. The global minimum geometry (GM) found by a conformational search was modified by breaking the O···U coordinative bond on the same side as the aromatic pendant. The resulting structure was optimized by a molecular mechanics method and then used as the starting geometry for a simulation in the temperature range of 323−423 K. Under the given conditions we did not observe enantiomerization, but quite an easy 360° rotation around the bond between the imine carbon atom and the disconnected phenoxide ring. Such a rotation leads, after O···U recombination, to the N-shaped intermediate **I** (Scheme 2, path B), whose energy is some 20 kcal mol^{-1} higher than that of GM. Rupture of the other O···U bond, followed by 360° rotation of the corresponding phenoxide ring, gives the other enantiomer, without the methyl group skipping over the dodecamethylene chain. This mechanism, as well as the previous one, is consistent with the measurement of almost identical barriers for compounds **3**−**5**.

A Configurationally Stable Inherently Chiral Uranyl−Salophen Complex. Although at present there are no conclusive experimental observations to definitely support either path A

(13) (a) Jeffrey, J. C.; Rauchfuss, T. B. *Inorg. Chem.* **1979**, *18*, 2658–2666. (b) Braunstein, P.; Naud, F. *Angew. Chem., Int. Ed.* **2001**, *40*, 680–699. (c) Bassetti, M. *Eur. J. Inorg. Chem.* **2006**, *70*, 4473–4482.

(14) If ligand hemilability does actually occur in salophen complexes, it must involve one of the O···U bonds, because rupture of a weaker N···U bond would require concomitant rupture of the adjacent O···U bond.

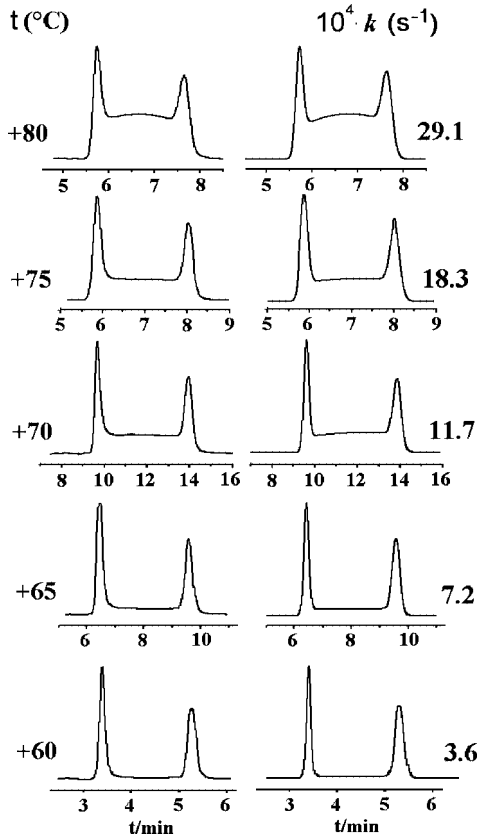

FIGURE 3. Temperature-dependent chromatograms of **3** on Chiralcel-OD column. Experimental profiles (left) vs calculated profiles (right) on the basis of the best first rate constants for enantiomerization (see Figure 2S within the Supporting Information for a superimposed view of experimental and simulated profiles).

TABLE 1. Activation Barriers $\Delta G^{\#}$ (kcal mol^{-1}) for the Enantiomerization of Compounds 3−5

T (°C)	3	4	5
60	24.83		25.10
65	24.74	24.92	25.11
70	24.79	24.91	25.23
75	24.85	24.84	25.22
80	24.89	24.83	25.28
mean $\Delta G^{\#}$	24.8 ± 0.1	24.9 ± 0.1	25.2 ± 0.1

or path B in Scheme 2, the hypothesis that the enantiomerization of inherently chiral uranyl−salophen macrocyclic complexes originates from ligand hemilability seems quite reasonable. Thus it was felt that an increase in the rigidity of the spacer should destabilize any intermediate involved in the enantiomerization process, thereby enhancing the enantiomerization half-life to such an extent that the use of uranyl−salophen complexes in enantioselective recognition and catalysis might become a practical proposition. On the basis of these considerations, we replaced the polymethylene chain of **3**−**5** with a more rigid spacer, i.e., the one derived from 4,4′-(1,4-phenylenediisopropylidene)bisphenol (bisphenol P), that appeared to meet the requirement of ensuring a high rigidity to the macrocyclic complex without compromising its formation and stability. A molecular dynamics investigation of compound **6** showed that a much higher temperature is required to achieve enantiomerization. This complex was prepared according to Scheme 3. Slow addition of a mixture of **11** and **12** to a solution of sodium hydride and bisphenol P in DMF was necessary to prevent

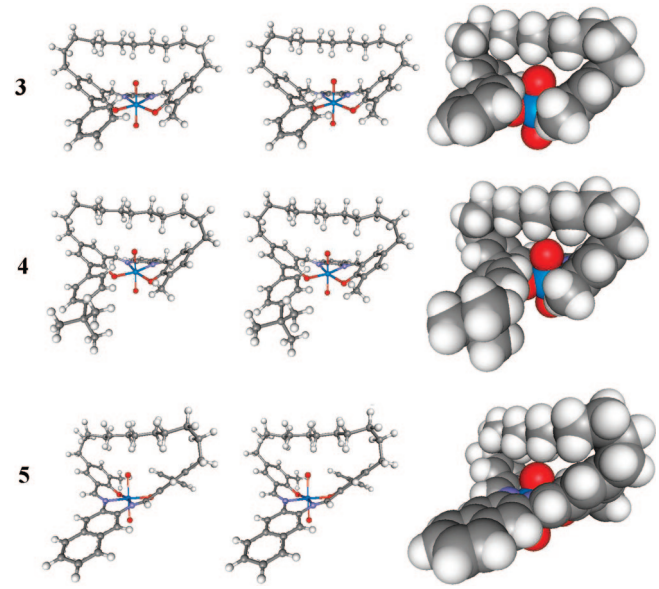

FIGURE 4. Ball and stick stereoview (left) and CPK (right) calculated structures of compounds **3**−**5**.

dimerization of the benzyl chlorides. Several attempts at resolving the statistical mixture of benzylated derivatives of bisphenol P were unsuccessful. Therefore, the crude product was subjected as such to macrocyclization under Ziegler's high dilution conditions. A pure sample of the desired nonsymmetrical compound **6** was obtained by flash chromatography. The two enantiomers of **6** were efficiently discriminated at 40 °C by enantioselective HPLC ($k_1' = 2.65$, $\alpha = 2.12$) on a Chiralcel-OD enantioselective column, using a ternary mixture of *n*-hexane/ethanol/methanol (60/30/10, v/v/v) as the mobile phase (Figure 5). When the temperature was increased above 80 °C, the appearance of an appreciable characteristic plateau zone between the two peaks still denoted the occurrence of a dynamic enantiomerization process concurrent with the chromatographic separation. The first-order enantiomerization rate constants, calculated by simulation of the chromatograms recorded at 80 and 90 °C, are given in Figure 6. These values correspond to $\Delta G^{\#}$ values of 26.64 and 26.99 kcal mol^{-1}, respectively,[15] which means that the energy barrier for enantiomerization of **6** is a couple of kilocalories per mole higher than that of **3** (Table 1). On the basis of the assumption that $\Delta G^{\#}$ is temperature independent, we calculate for **6** an enantiomerization half-life of 61 d at room temperature, a value that is 32, 27, and 16 times higher than those calculated for **3**, **4**, and **5**, respectively.

These experimental results, while offering support to the hypothesis that enantiomerization in uranyl−salophen complexes implies a ligand hemilability phenomenon, clearly establish that compound **6**, easily obtainable in enantiomerically pure form by semipreparative enantioselective HPLC, represents the first

(15) As suggested by a reviewer, one strongly enriched enantiomer of **6**, obtained from semipreparative chromatographic enantioseparation of a small sample of racemic **6** (CHIRALPAK IA, 250 × 100 mm i.d., chiral stationary phase; mobile phase *n*-hexane/CH_2Cl_2/MeOH 60:10:30 v/v/v), was subjected to classical determination of the enantiomerization kinetics under homogeneous conditions in the solvent mixture (*n*-hexane/EtOH/MeOH 60:30:10 v/v/v) used in the dynamic HPLC measurements. Racemization was monitored as a function of time by analytical enantioselective chromatography at 20 °C. A value of 7.5 × 10^{-5} s^{-1} was determined for the enantiomerization rate constant at 65 °C, which corresponds to an activation barrier of $\Delta G^{\neq} = 26.26$ kcal mol^{-1}. This value compares fairly well with the values determined by dynamic HPLC, showing that major contributions to enantiomerization from the stationary phase are very unlikely.

SCHEME 2. Enantiomerization of Uranyl−Salophen Complex 3 Based on Ligand Hemilability via the One-Step Mechanism (path A) and via a Two-Step Mechanism (path B)[a]

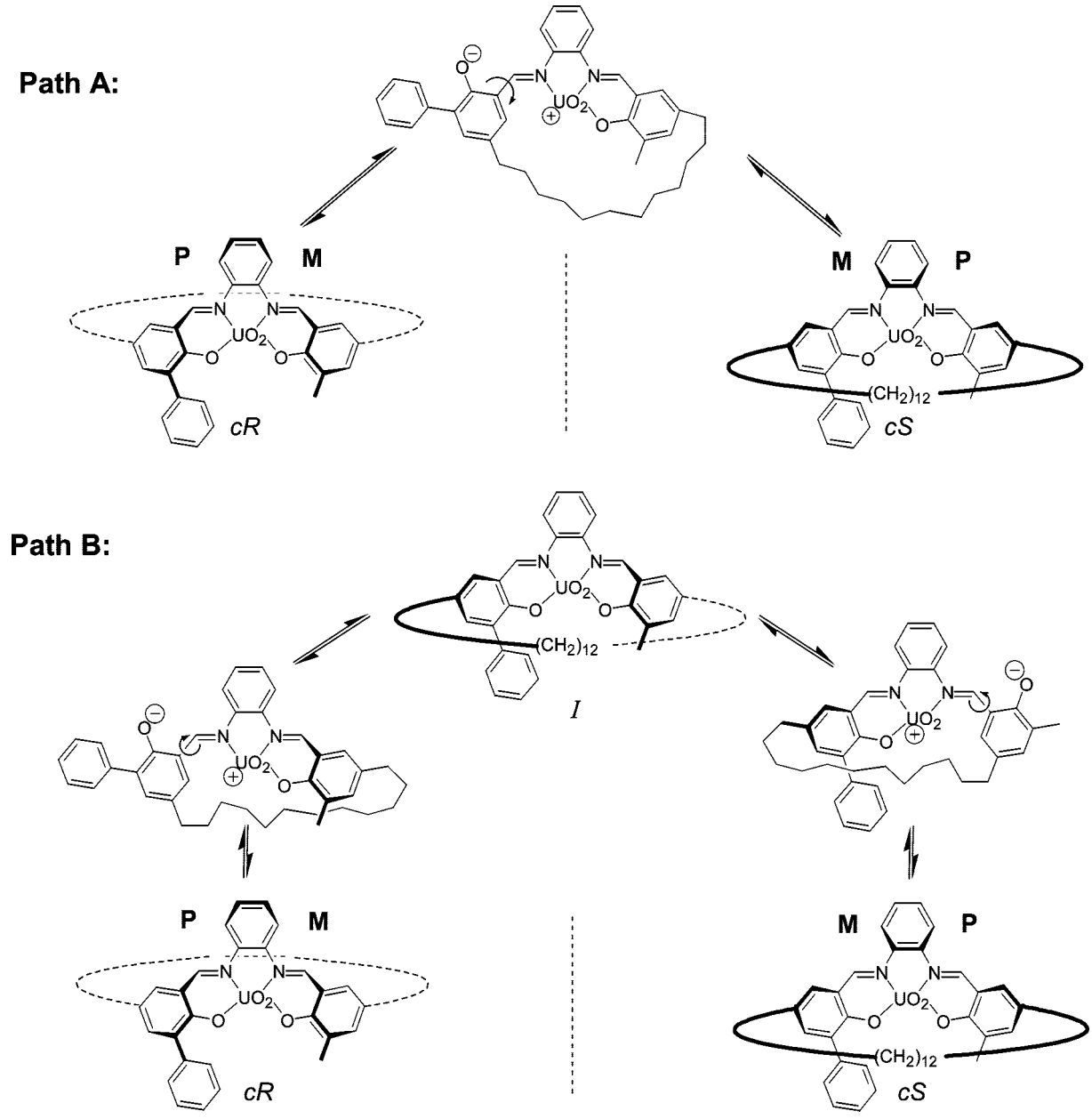

[a] For the *c*R-*c*S chirality descriptors see ref 9.

member of a new family of inherently chiral receptors whose potential in chiral recognition and catalysis actually can be explored.

Experimental Section

Solvents and chemicals were used as received unless otherwise stated. 2-Hydroxy-3-phenylbenzaldehyde was available from a previous work.[6e]

4′-*tert*-Butyl-2-methoxy-1,1′-biphenyl. A solution of p-*tert*-butylbromobenzene (1.50 g, 7.0 mmol) and $Pd(PPh_3)_4$ (0.152 g, 0.131 mmol) in 23 mL of anhydrous toluene was added to a solution of 2-methoxyphenylboronic acid (1.34 g, 8.82 mmol) in 20 mL of absolute ethanol under argon atmosphere, followed by addition of K_2CO_3 (2.15 g, 15.5 mmol). The mixture was stirred and heated to reflux for 20 h and allowed to cool to room temperature. NaOH (55 mL, 0.5 M solution) was added and the mixture was extracted twice with 30 mL portions of CH_2Cl_2. The organic layers were combined, washed with 25 mL of H_2O, and dried over Na_2SO_4. Chromatographic purification of the crude product (silica gel, 2% ethyl acetate in hexanes) afforded 4′-*tert*-butyl-2-methoxybiphenyl as a colorless oil (1.48 g, 88% yield). ^1H NMR (200 MHz, $CDCl_3$) δ 7.54−7.42 (m, 4H), 7.35−7.28 (m, 2H), 7.05−6.97 (m, 2H), 3.82 (s, 3H), 1.36 (s, 9H) ppm.

1-(6-Methoxy-1,1′-biphenyl-3-yl)-12-(3-methyl-4-methoxyphenyl)dodecane-1,12-dione (7a). $AlCl_3$ (2.29 g, 17.2 mmol) and CH_2Cl_2 (2.0 mL) were placed under argon atmosphere in a dry flask cooled with an ice bath. A solution of dodecanedioic acid dichloride (2.19 g, 8.19 mmol) in CH_2Cl_2 (2.0 mL) was added. 2-Methylanisole (1.00 g, 8.19 mmol) and 2-methoxy-1,1′-biphenyl (1.51 g, 8.19 mmol) in CH_2Cl_2 (2.0 mL) were slowly added and finally the mixture was diluted with CH_2Cl_2 (2.0 mL) and stirred for 40 min at room temperature. The resulting mixture was slowly poured into ice cold 6 M hydrochloric acid (20 mL) and CH_2Cl_2

SCHEME 3. Synthetic Procedure for Compound 6[a]

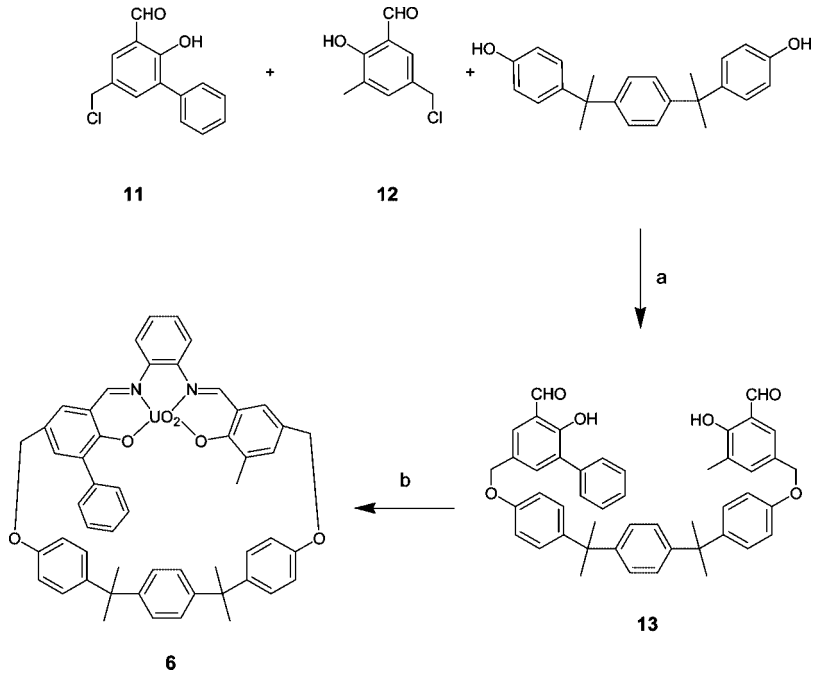

[a] Reagents and conditions: (a) NaH, DMF; (b) 1,2-diaminobenzene, $UO_2(OAc)_2 \cdot 2H_2O$, CH_3OH.

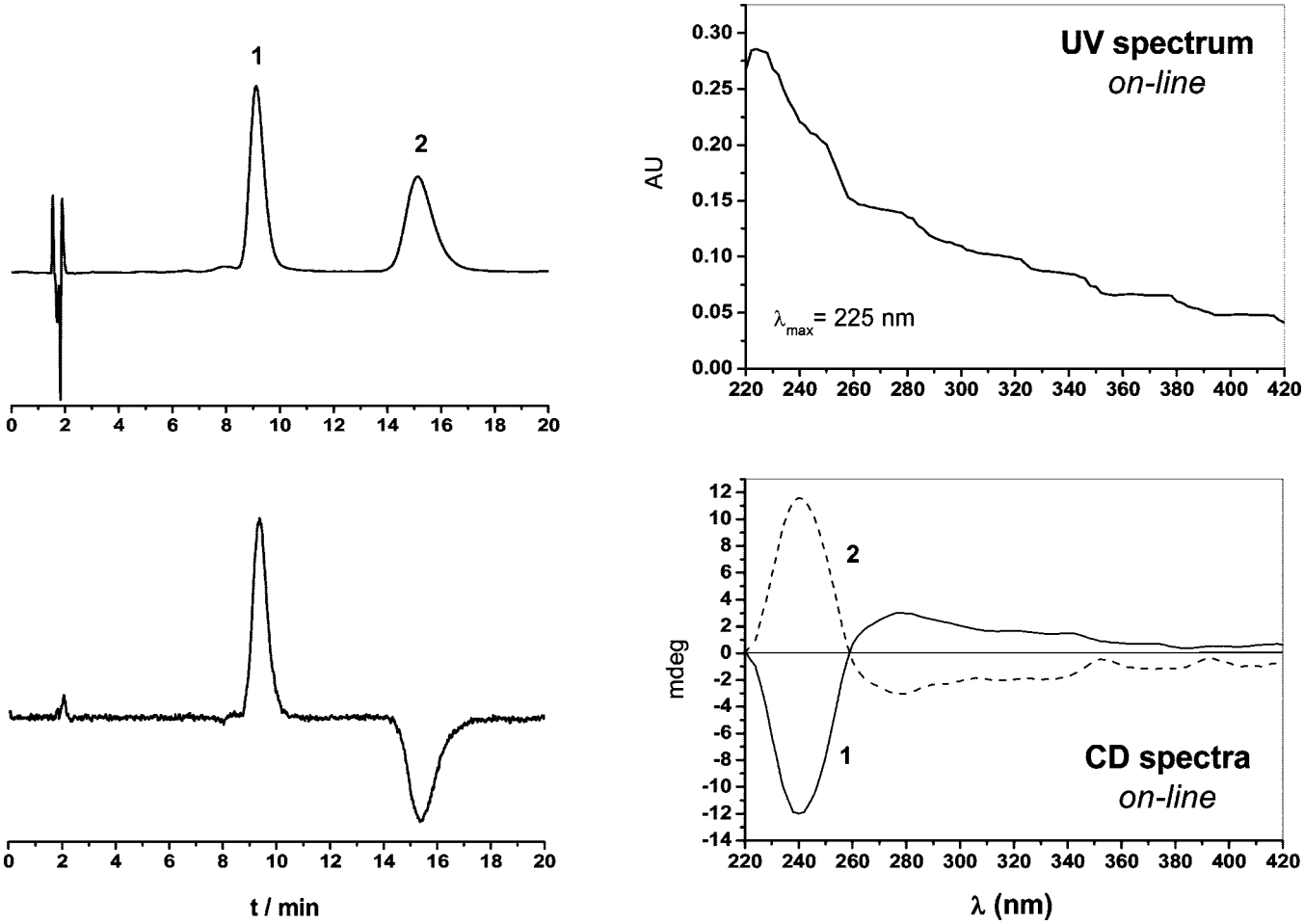

FIGURE 5. Analytical separation of the enantiomers of **6** by enantioselective HPLC at 25 °C. UV (top) and CD (bottom) chromatographic traces at 400 nm (left) and corresponding *online* spectra (right).

(15 mL) was added. The organic layer was washed twice with 20 mL of $NaHCO_3$ (sat.) and then with 20 mL of brine, then it was dried over anhydrous sodium sulfate. Chromatographic purification of the crude product (silica gel, 5% acetone and 10% $CHCl_3$ in

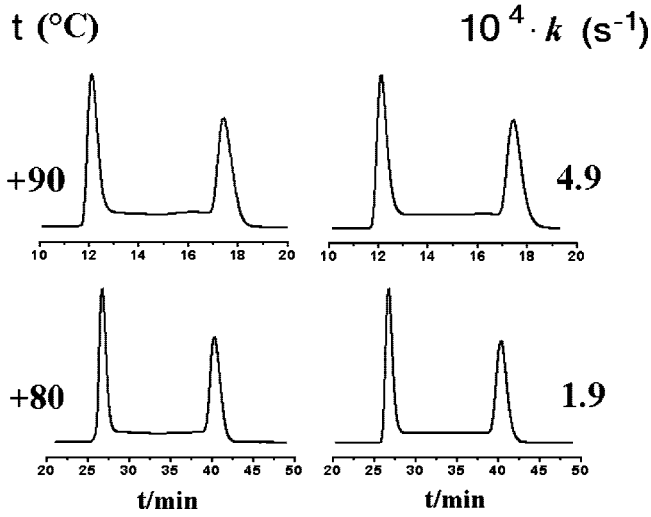

FIGURE 6. Temperature-dependent chromatograms of **6** on Chiralcel-OD column. Experimental profiles (left) vs calculated profiles (right) on the basis of the best first rate constants for the enantiomerization. (see Figure 3S in the Supporting Information for a superimposed view of experimental and simulated profiles).

hexanes) afforded **7a** as a colorless oil (1.08 g, 24% yield). Elemental Anal. Calcd (%) for $C_{33}H_{40}O_4$: C, 79.16; H, 8.05. Found: C, 79.25; H, 7.94. ^{1}H NMR (200 MHz, $CDCl_3$) δ 7.98−7.77 (m, 4H), 7.53−7.34 (m, 5H), 7.00 (d, 1H, J = 8.48 Hz), 6.83 (d, 1H, J = 8.48 Hz), 3.88 (s, 6H), 2.96−2.85 (m, 4H), 2.23 (s, 3H), 1.75−1.66 (m, 4H), 1.38−1.24 (m, 12H) ppm. ^{13}C NMR (50 MHz, $CDCl_3$) δ 200.3, 200.0, 162.2, 160.9, 138.3, 131.9, 131.4, 131.3, 130.9, 130.4, 130.2, 130.1, 128.8, 128.1, 127.4, 111.3, 109.9, 56.5, 56.2, 39.0, 38.9, 30.1, 25.4, 25.3, 17.0 ppm. MS-ESI-TOF for $C_{33}H_{40}O_4$ 500.29, found 523.6 ([M + Na]$^+$).

1-(6-Methoxy-1,1′-biphenyl-3-yl)-12-(3-methyl-4-methoxyphenyl)dodecane (8a). Compound **7a** (0.125 g, 0.250 mmol) was dissolved in 2.5 mL of 1,2-dichloroethane. ZnI_2 (0.239 g, 0.749 mmol) and $NaCNBH_3$ (0.235 g, 3.94 mmol) were added in the given order and the reaction mixture was stirred at room temperature for 20 h. The mixture was then filtered on a celite plug that was washed thoroughly with dichloromethane. Evaporation of the solvent afforded the desired product as a colorless oil in quantitative yield. ^{1}H NMR (200 MHz, $CDCl_3$) δ 7.59 (br d, 2H, J = 7.25 Hz), 7.46 (br t, 2H), 7.38 (m, 1H), 7.20−7.16 (m, 2H), 7.01 (m, 2H), 6.95 (d, 1H, J = 8.12 Hz), 6.78 (d, 1H, J = 8.78 Hz), 3.85 (s, 3H), 3.83 (s, 3H), 2.65 (t, 2H, J = 7.68 Hz), 2.57 (t, 2H, J = 7.90 Hz), 2.27 (s, 3H), 1.65−1.63 (m, 4H), 1.37−1.33 (m, 16H) ppm. ^{13}C NMR (50 MHz, $CDCl_3$) δ 156.4, 155.2, 139.4, 135.9, 135.3, 131.6, 131.4, 131.1, 130.2, 128.9, 128.6, 127.5, 127.0, 126,9, 111.8, 110.5, 56.3, 56.0, 35.8, 35.7, 30.2, 30.0, 16.9 ppm. MS-ESI-TOF for $C_{33}H_{44}O_2$ 472.33, found 495.5 ([M + Na]$^+$).

1-(6-Hydroxy-1,1′-biphenyl-3-yl)-12-(3-methyl-4-hydroxyphenyl)dodecane (9a). Compound **8a** (0.119 g, 0.250 mmol) and dry toluene (3.0 mL) were placed under an argon atmosphere in a dry flask. A solution of boron tribromide (0.062 mL, 0.66 mmol) in dry toluene (3.0 mL) was added dropwise to the stirred solution cooled at 0 °C. The reaction mixture was stirred for 24 h at room temperature, then cooled again in an ice bath, and then water (40 mL) was added. The solution was extracted with 3 portions of diethyl ether (30 mL each), then the combined organic layers were washed twice with 20 mL of water and dried over anhydrous sodium sulfate. Evaporation of the solvent afforded **9a** as a dark brown oil pure enough to be used as such in the following step (0.113 g, 96% yield). ^{1}H NMR (200 MHz, $CDCl_3$) δ 7.46−7.27 (m, 4H), 7.22−7.04 (m, 3H), 6.91−6.85 (m, 3H, J = 8.12 Hz), 6.66 (d, 1H, J = 8.03 Hz), 5.29 (s, 2H), 2.55 (t, 2H, J = 7.68 Hz), 2.48 (t, 2H, J = 7.90 Hz), 2.21 (s, 3H), 1.59−1.52 (m, 4H), 1.28−1.18 (m, 16H) ppm. ^{13}C NMR (50 MHz, $CDCl_3$) δ 152.4, 151.0, 138.2, 136.1, 135.9, 131.7, 130.8, 130.0, 129.9, 129.7, 129.0, 128.5, 127.5, 124.1, 116.3, 115.4, 35.9, 35.8, 32.6, 32.5, 30.5, 30.4, 30.3, 30.1, 16.0 ppm. MS-ESI-TOF for $C_{31}H_{40}O_2$ 444.30, found 467.4 ([M + Na]$^+$).

1-(5-Formyl-6-hydroxy-1,1′-biphenyl-3-yl)-12-(3-formyl-4-hydroxy-5-methylphenyl)dodecane (10a). Compound **9a** (0.880 g, 1.98 mmol) was dissolved in dry dichloromethane (70 mL) and placed under an argon atmosphere in a dry two-necked flask together with α,α′-dichloromethyl methyl ether (4.6 mL, 51.5 mmol). Titanium tetrachloride (2.6 mL, 23 mmol) was added dropwise over 20 min to the stirred solution cooled at 0 °C. After 2 h, the reaction mixture was diluted with water (300 mL). The aqueous layer was extracted with 2 portions of dichloromethane (200 mL each). The combined organic layers were washed twice with 150 mL of water, dried over anhydrous sodium sulfate, and concentrated to afford an oil that was purified by flash chromatography (silica gel, 5% ethyl acetate in hexanes) to give the desired product as a pale yellow oil (0.180 g, 18% yield). Elemental Anal. Calcd (%) for $C_{33}H_{40}O_4$: C, 79.16; H, 8.05. Found: C, 79.20; H, 7.96. ^{1}H NMR (200 MHz, $CDCl_3$) δ 11.34 (s, 1H), 11.08 (s, 1H), 9.91 (s, 1H), 9.83 (s, 1H), 7.59−7.57 (m, 2H), 7.44−7.33 (m, 5H), 7.20−7.15 (m, 2H), 2.62 (t, 2H, J = 7.63 Hz), 2.53 (t, 2H, J = 7.90 Hz), 2.24 (s, 3H), 1.67−1.51 (m, 4H), 1.29−1.25 (m, 16H) ppm. ^{13}C NMR (50 MHz, $CDCl_3$) δ 197.5, 197.4, 158.8, 157.7, 139.1, 139.0, 137.2, 135.0, 134.4, 133.0, 131.0, 130.9, 130.0, 128.9, 128.3, 127.2, 121.3, 120.4, 35.5, 35.4, 32.2, 32.1, 30.3, 30.2, 30.1, 29.9, 15.7 ppm. MS-ESI-TOF for $C_{33}H_{40}O_4$ 500.29, found 523.9 ([M + Na]$^+$).

1-(4′-*tert*-Butyl-5-formyl-6-hydroxy-1,1′-biphenyl-3-yl)-12-(3-formyl-4-hydroxy-5-methylphenyl)dodecane (10b). $AlCl_3$ (0.707 g, 5.31 mmol) and CH_2Cl_2 (0.7 mL) were placed under argon atmosphere in a dry flask cooled with an ice bath. A solution of dodecanedioic acid dichloride (0.549 g, 2.05 mmol) in CH_2Cl_2 (0.7 mL) was added. 2-Methylanisole (0.255 g, 2.08 mmol) and 4′-*tert*-butyl-2-methoxy-1,1′-biphenyl (0.505 g, 2.10 mmol) in CH_2Cl_2 (1.0 mL) were slowly added and finally the mixture was diluted with CH_2Cl_2 (1.0 mL) and stirred for 150 min at room temperature. The resulting mixture was slowly poured into ice cold 6 M hydrochloric acid (10 mL) and CH_2Cl_2 (5 mL) was added. The organic layer was washed twice with 10 mL of $NaHCO_3$ (sat.) and then with 10 mL of brine, then it was dried over anhydrous sodium sulfate. Chromatographic treatment of the crude product (silica gel, 3% acetone, and 15% $CHCl_3$ in hexanes) allowed the recovery of 0.424 g of a mixture of product **7b** and its symmetrical byproduct. Since all attempts were unsuccessful, no further purification was carried on. This mixture was then dissolved in 8.0 mL of 1,2-dichloroethane. ZnI_2 (0.729 g, 2.28 mmol) and $NaCNBH_3$ (0.718 g, 11.4 mmol) were added in the given order and the reaction mixture was stirred at room temperature for 22 h, after which it was filtered on a celite plug that was washed thoroughly with dichloromethane. Evaporation of the solvent afforded 0.4 g of a mixture of **8b** and the corresponding symmetrical products. Since even at this stage all attempts at further purification were unsuccessful, this mixture was used as is, dissolved in dry toluene (5.0 mL), and placed under an argon atmosphere in a dry flask. A solution of boron tribromide (0.18 mL, 1.9 mmol) in dry toluene (5.0 mL) was added dropwise to the stirred solution cooled at 0 °C The reaction mixture was stirred for 23 h at room temperature, then cooled again in an ice bath and water (50 mL) was added. The solution was extracted with 3 portions of diethyl ether (40 mL each), the combined organic layers were washed twice with 30 mL of water and dried over anhydrous sodium sulfate. Evaporation of the solvent afforded a mixture of **9b** and its symmetrical counterparts that was again used as such in the following step. The above mixture (0.880 g, 1.98 mmol) was dissolved in dry dichloromethane (70 mL) and placed under an argon atmosphere in a dry two-necked flask together with α,α′-dichloromethyl methyl ether (4.6 mL, 51.5 mmol). Titanium tetrachloride (2.6 mL, 23 mmol) was added dropwise over 20 min to the stirred solution that was cooled at 0 °C. After 2 h, the reaction

mixture was diluted with water (300 mL). The aqueous layer was extracted with 2 portions of dichloromethane (200 mL each). The combined organic layers were washed twice with 150 mL of water, dried over anhydrous sodium sulfate, and concentrated to afford an oil that was purified by flash chromatography (silica gel, 5% ethyl acetate in hexane) to give the desired product as a pale yellow oil (0.180 g, 18% yield). Elemental Anal. Calcd (%) for $C_{37}H_{48}O_4$: C, 79.82; H, 8.69. Found: C, 79.93; H, 8.55. ^{1}H NMR (200 MHz, $CDCl_3$) δ 11.40 (s, 1H), 11.14 (s, 1H), 9.96 (s, 1H), 9.87 (s, 1H), 7.62−7.20 (m, 8H), 2.71−2.55 (m, 4H), 2.29 (s, 3H), 1.68−1.50 (m, 4H), 1.40−1.24 (m, 25H) ppm. ^{13}C NMR (50 MHz, $CDCl_3$) δ 197.6, 197.5, 158.8, 157.7, 139.2, 139.0, 135.1, 134.5, 133.1, 132.3, 131.1, 130.0, 129.9, 129.6, 128.3, 127.2, 120.5, 35.5, 32.3, 30.5, 30.3, 30.2, 29.9, 15.8 ppm. MS-ESI-TOF for $C_{37}H_{48}O_4$ 556.77, found 579.8 ($[M + Na]^+$).

Complex 3. A solution of **10a** (0.064 g, 0.128 mmol) in dichloromethane (2.5 mL) and a solution of 1,2-diaminobenzene (0.0138 g, 0.127 mmol) in a 1:1 mixture of methanol and dichloromethane (2.5 mL) were added separately and simultaneously by a syringe pump over 5.5 h to a solution of uranyl acetate (0.055 g, 0.129 mmol) in methanol (100 mL). Formation of a red precipitate was observed. The mixture was left to stand overnight at room temperature and then concentrated to a volume of 10 mL and dissolved again in dichloromethane (100 mL). The organic phase was extracted with 2 portions of a saturated solution of $NaHCO_3$ (50 mL each), washed to neutrality with 2 portions of water (40 mL each), dried over anhydrous sodium sulfate, and concentrated to afford a dark red product that was purified by flash chromatography (silica gel, 30% acetone in cyclohexane) to give the desired products as a dark red solid (0.060 g, 56% yield). Elemental Anal. Calcd (%) for $C_{39}H_{42}N_2O_4U\cdot 3H_2O$: C, 52.35; H, 5.41; N, 3.13. Found: C, 52.63; H, 5.28; N, 3.33. ^{1}H NMR (200 MHz, acetone-d_6) δ 9.43 (s, 1H), 9.38 (s, 1H), 7.86−7.73 (m, 4H), 7.60−7.40 (m, 7H), 7.29 (br m, 1H), 7.21 (br m, 1H), 2.69−2.64 (m, 2H), 2.58−2.54 (m, 2H), 2.39 (s, 3H), 1.62−1.08 (m, 20H) ppm. ^{13}C NMR (75 MHz, acetone-d_6) δ 167.6, 167.4, 147.6, 140.5, 137.4, 133.8, 131.6, 131.5, 130.8, 130.4, 129.4, 129.3, 128.3, 126.8, 124.6, 122.8, 119.6, 34.5, 33.0, 32.2, 31.9, 31.8, 31.8, 28.3, 27.0, 16.4 ppm. MS-ESI-TOF for $C_{39}H_{42}N_2O_4UNa^+$ calcd 863.36, found 863.32.

Complex 4. Preparation was accomplished following the same procedure as described for **3** and replacing **10a** with **10b**. The desired product was purified by flash chromatography (silica gel, 20% ethyl acetate in cyclohexane) to give the desired products as a dark red solid in a 38% yield. Elemental Anal. Calcd (%) for $C_{43}H_{50}N_2O_4U\cdot 3H_2O$: C, 54.31; H, 5.94; N, 2.95. Found: C, 54.55; H, 6.06; N, 2.79. ^{1}H NMR (200 MHz, acetone-d_6) δ 9.44 (s, 1H), 9.39 (s, 1H), 7.88−7.23 (m, 12H), 2.65−2.51 (m, 4H), 2.39 (s, 3H), 1.71−1.10 (m, 29H) ppm. ^{13}C NMR (75 MHz, acetone-d_6) δ 167.8, 167.7, 147.7, 147.3, 137.4, 134.0, 133.0, 131.4, 130.5, 130.0, 129.5, 129.4, 128.4, 128.1, 127.0, 124.8, 123.3, 123.2, 122.4, 119.8, 119.7, 35.8, 35.4, 35.2, 34.9, 34.7, 32.4, 32.0, 30.7, 26.7, 23.5, 23.0, 22.9, 22.5, 22.3, 16.3 ppm. MS-ESI-TOF for $C_{43}H_{50}N_2O_4UNa^+$ calcd 919.42, found 919.15.

Complex 5. Preparation was accomplished following the same procedure as described for **3** and replacing 1,2-diaminobenzene with 2,3-diaminonaphthalene. The desired product was purified by flash chromatography (silica gel, 20% ethyl acetate in cyclohexane) to give the desired products as a dark red solid in a 62% yield. Elemental Anal. Calcd (%) for $C_{43}H_{44}N_2O_4U\cdot 3H_2O$: C, 54.66; H, 5.33; N, 2.96. Found: C, 54.48; H, 5.59; N, 3.14. ^{1}H NMR (200 MHz, acetone-d_6) δ 9.62 (s, 1H), 9.56 (s, 1H), 8.22−7.86 (m, 4H), 7.87 (br d, 2H), 7.56−7.26 (m, 9H), 2.69−2.56 (m, 4H), 2.42 (s, 3H), 1.80−1.10 (m, 20H) ppm. ^{13}C NMR (75 MHz, acetone-d_6) δ 167.4, 167.3, 147.6, 147.3, 139.4, 139.0, 137.5, 137.0, 134.6, 132.4, 132.0, 130.8, 130.5, 130.4, 129.3, 129.2, 128.3, 128.0, 127.7, 126.9, 125.4, 125.0, 124.4, 122.8, 117.7, 117.6, 35.1, 34.9, 31.4, 30.9, 30.5, 30.4, 28.0, 16.2 ppm. MS-ESI-TOF for $C_{43}H_{44}N_2O_4UNa^+$ calcd 913.37, found 913.49.

5-Chloromethyl-2-hydroxy-3-phenylbenzaldehyde (11). 2-Hydroxy-3-phenylbenzaldehyde (0.402 g, 2.03 mmol) was dissolved in a mixture of dioxane (3.6 mL), glacial acetic acid (0.760 mL), 85% phosphoric acid (0.760 mL), and 35% hydrochloric acid (36.4 mL). *p*-Formaldehyde (1.21 g, 40.3 mmol) was added and the reaction mixture was stirred at 80 °C for 24 h, after which time H_2O (25 mL) and dichloromethane (25 mL) were added. The organic phase was washed with H_2O until neutrality and dried over sodium sulfate. Evaporation of the solvent afforded the desired product as a colorless oil (0.500 g, 100% yield). Elemental Anal. Calcd (%) for $C_{14}H_{11}ClO_2$: C, 68.16; H, 4.49. Found: C, 68.07; H, 4.71. ^{1}H NMR (200 MHz, $CDCl_3$) δ 11.58 (s, 1H), 9.94 (s, 1H), 7.64−7.38 (m, 7H), 4.63 (s, 2H) ppm. ^{13}C NMR (50 MHz, $CDCl_3$) δ 196.4, 158.9, 138.0, 135.6, 132.8, 131.2, 129.6, 129.2, 128.3, 124.6, 120.6, 45.2 ppm. GC-MS *m*/*z* (+) 211 (M^+ − Cl, 100%).

5-Chloromethyl-2-hydroxy-3-methylbenzaldehyde (12). 2-Hydroxy-3-methylbenzaldehyde (1.10 mL, 9.07 mmol), formaldehyde 37 wt % in H_2O (0.7 mL), and concentrated hydrochloric acid (9.5 mL) were mixed and stirred overnight. The solid that separated from the reaction mixture was filtered, dissolved in diethyl ether, and dried over sodium sulfate. Recrystallization from light petroleum afforded **12** in 65% yield (mp 76−77 °C, lit.[16] mp 81.5−82.5). ^{1}H NMR (200 MHz, $CDCl_3$) δ 11.31 (s, 1H), 9.86 (s, 1H), 7.42 (br s, 2H), 4.55 (s, 2H), 2.27 (s, 3H) ppm.

Complex 6. Sodium hydride 60% dispersion in mineral oil (1.78 g, 44.5 mmol) was placed under argon atmosphere in a dry flask, washed three times with *n*-hexane, and suspended in anhydrous DMF (9 mL). 4-(1-{4-[1-(4-Hydroxyphenyl)-1-methylethyl]phenyl}-1-methylethyl)phenol (0.843 g, 2.43 mmol) was slowly added. After the evolution of hydrogen had ceased, a solution of **11** (0.599 g, 2.44 mmol) and **12** (0.450 g, 2.44 mmol) in DMF (7 mL) was slowly added by a syringe pump over 24 h. The resulting yellow solution was gently poured over ice, acidified with concentrated hydrochloric acid to pH 3−4, and extracted with two 25 mL portions of dichloromethane. The organic layers were collected, washed with brine, and dried over anhydrous sodium sulfate. Chromatographic treatment of the crude product (silica gel, toluene) afforded 0.940 g of a mixture of product **13** and its symmetrical counterparts. Since all attempts were unsuccessful, no further purification was carried on. A solution of this mixture in dichloromethane (60 mL) and a solution of 1,2-diaminobenzene (0.159 g, 1.47 mmol) in a 1:1 mixture of methanol and dichloromethane (60 mL) were added separately and simultaneously by syringe pump over 24 h to a solution of uranyl acetate (0.725 g, 1.71 mmol) in methanol (380 mL). The reaction mixture was filtered to remove an orange precipitate containing the higher oligomers of the desired product, concentrated to a volume of 100 mL, and diluted with dichloromethane (250 mL). The organic phase was washed to

(16) Stoermer, R.; Behn, K. *Chem. Ber.* **1901**, *34*, 2455–2460.

(17) (a) QCPE program No. 633 by Martin Jung, Indiana University, Bloomington, IN, 1991. (b) Trapp, O.; Schurig, V. *Comp. Chem.* **2001**, *25*, 187−195.

(18) (a) Gasparrini, F.; Lunazzi, L.; Mazzanti, A.; Pierini, M.; Pietrusiewicz, K. M.; Villani, C. *J. Am. Chem. Soc.* **2000**, *122*, 4776–4780. (b) Dell'Erba, C.; Gasparrini, F.; Grilli, S.; Lunazzi, L.; Mazzanti, A.; Novi, M.; Pierini, M.; Tafani, C.; Villani, C. *J. Org. Chem.* **2002**, *67*, 1663–1668. (c) Gasparrini, F.; Grilli, S.; Leardini, R.; Lunazzi, L.; Mazzanti, A.; Nanni, D.; Pierini, M.; Pinamonti, M. *J. Org. Chem.* **2002**, *67*, 3089–3095. (d) Dalla Cort, A.; Gasparrini, F.; Lunazzi, L.; Mandolini, L.; Mazzanti, A.; Pasquini, C.; Pierini, M.; Rompietti, R.; Schiaffino, L. *J. Org. Chem.* **2005**, *70*, 8877–8883. (e) Cirilli, R.; Ferretti, R.; La Torre, F.; Secci, D.; Bolasco, A.; Carradori, S.; Pierini, M. *J. Chromatogr. A* **2007**, *117*, 160–169.

(19) (a) Giddings, J. C. *J. Chromatogr.* **1960**, *3*, 443–453. (b) Kramer, R. *J. Chromatogr.* **1975**, *107*, 241–252. (c) Schurig, V.; Burkle, W. *J. Am. Chem. Soc.* **1982**, *104*, 7573–7580. (d) Burkle, W.; Karfunkel, H.; Schurig, V. *J. Chromatogr.* **1984**, *288*, 1–14. (e) Veciana, J.; Crespo, M. I. *Angew. Chem., Int. Ed. Engl.* **1991**, *30*, 74–77. (f) Trapp, O.; Schoetz, G.; Schurig, V. *Chirality* **2001**, *13*, 403–414. (g) Trapp, O. *Anal. Chem.* **2006**, *78*, 189–198. (h) Oxelbark, J.; Allenmark, S. *J. Chem. Soc., Perkin Trans. 2* **1999**, *8*, 1587–1590. (i) Wolf, C. *Chem. Soc. Rev.* **2005**, *34*, 595–608. (j) Cabrera, K.; Jung, M.; Fluck, M.; Schurig, V. *J. Chromatogr. A* **1996**, *731*, 315–321. (k) Trapp, O.; Schurig, V. *Chirality* **2002**, *14*, 465–470. (l) Trapp, O.; Trapp, G.; Schurig, V. *J. Biochem. Biophys. Methods* **2002**, *54*, 301–313.

neutrality with 3 portions of water (200 mL each) and dried over anhydrous sodium sulfate. The crude product was purified twice by flash chromatography (silica gel, 15% acetone in cyclohexane) to give the desired product as a red solid (0.041 g, 1.6% yield). Elemental Anal. Calcd (%) for $C_{53}H_{46}N_2O_4U\cdot 3H_2O$: C, 57.92; H, 4.77; N, 2.55. Found: C, 57.79; H, 4.95; N, 2.70. ^{1}H NMR (300 MHz, $CDCl_3$) δ 9.30 (s, 1H), 9.27 (s, 1H), 7.86−7.49 (m, 12H), 6.95−6.56 (m, 13H), 5.35 (d, 1H, J = 13.8 Hz), 5.27 (d, 1H, J = 13.6 Hz), 5.07−4.96 (m, 2H), 2.54 (s, 3H), 1.49−1.41 (m, 12H) ppm. ^{13}C NMR (50 MHz, $CDCl_3$) δ 166.8, 166.6, 156.1, 148.1, 148.0, 147.1, 146.9, 142.1, 141.9, 139.6, 136.4, 135.9, 133.8, 132.5, 131.9, 130.5, 129.8, 129.6, 129.4, 128.7, 128.3, 127.6, 127.4, 126.6, 126.3, 124.3, 122.7, 119.7, 119.6, 114.4, 114.3, 68.7, 68.5, 42.2, 31.9, 31.8, 31.2, 17.2 ppm. MS-ESI-TOF for $C_{53}H_{446}N_2O_6U$ calcd 1044.39, found 1045.20 ([M + H$^+$]), 1067.12 ([M + Na$^+$]), 1083.18 ([M + K$^+$]).

Chromatography. Analytical liquid chromatography was performed on a chromatograph equipped with a Rheodyne model 7725i 20 μL loop injector, PU-1580-CO_2 and PU-980 Jasco HPLC pumps, and a Jasco 995-CD chiro-optical UV/CD detector. Chromatographic data were collected and processed with Jasco Borwin software.

Enantioseparations were performed on a Chiralcel-OD column, using *n*-hexane/ethanol/$CHCl_3$ (50/30/20, v/v/v, for **3** and **4**; 55/30/15, v/v/v, for **5**) and *n*-hexane/ethanol/methanol (60/30/10, v/v/v, for **6**) as the mobile phases at different flow rates with UV detection at 400 nm. Chiralcel-OD (cellulose tris(3,5-dimethyl phenylcarbamate) coated on a 5 μm mesoporous silica gel column (250 × 4.6 mm, L × i.d.)) was obtained from Chiral Technologies. Variable-temperature chromatography with UV and CD detection was performed by placing the column inside a homemade thermally insulated container cooled by the expansion of liquid carbon dioxide. The flow of liquid CO_2 and the column temperature were regulated by a solenoid valve, a thermocouple, and an electric controller. Temperature variations after thermal equilibration were within ±0.1 °C.

Dynamic High Performance Liquid Chromatography (DHPLC). Reproducibility of all variable-temperature experimental chromatograms (VTECs) employed in on-column rate constants determinations was checked by comparing the retention times registered within three independent injections at identical conditions. Simulation of VTECs was performed by use of the dedicated home made computer program Auto DHPLC y2k (Auto Dynamic HPLC), which implements both stochastic and theoretical plates models according to mathematical equations and procedures described in refs 17a and 17b, respectively. The implemented algorithm may take into account all types of first-order interconversions, i.e., enantiomerizations as well as diastereomerizations or constitutional isomerizations (e.g., pseudo-first-order tautomerizations). Program functionality was validated on several first-order isomerizations (both enantiomerizations and nonenantiomerizations) by comparing DHPLC results with the equivalent ones obtained by DNMR technique[18a–d] or classical method.[18e] The used algorithm also allows for taking tailing effects into account. Both chromatographic (retention times, number of theoretical plates, peaks' tailing) and kinetic parameters (apparent rate constants) can be automatically optimized by simplex procedure to obtain the best agreement between experimental and simulated dynamic chromatograms. In the present paper all simulations were performed employing the stochastic model and taking into account tailing effects. The agreement between experimental and simulated dynamic chromatograms was quantitatively evaluated as root-mean-square differences (rmsd) between the two normalized chromatograms. Rmsd minimizations were obtained refining both chromatographic and kinetic parameters by simplex procedure working in automatic fashion. In all cases, simulations were run until achievement of rmsd convergence in the simplex procedure (rmsd gradient $<1\times10^{-4}$). Errors associated with the so evaluated rate constants were estimated to be lower than 2%. Calculations of $\Delta G^{\#}$ barriers related to enantiomerization equilibria of compounds **3**, **4**, **5**, and **6** were performed by inserting the apparent enantiomerization rate constants k determined by DHPLC simulations at the suitable temperatures into the Eyring equation:

$$\Delta G^{\#} = RT\ln\frac{\gamma k_B T}{hk}$$

where k_B is the Boltzmann constant, T is temperature, R is the gas constant, h is the Planck constant, γ is the transmission factor, and k is the rate constant. In all calculations the transmission factor γ was set to 1. A quite comprehensive view of both fundamental works concerning principles on which dynamic chromatography is based on and applications of the dynamic chromatography technique to the study enantiomerization processes is given in ref 19.

Computational Methods. Molecular modeling calculations were performed by the program HyperChem Professional for Windows OS, release 7.5, running on a PC equipped with Intel Pentium 4, CPU 3.40 GHz, 2 GB of RAM, and OS Windows 2000 Professional. The conformational search of compounds **3** and **6** was carried out by using the following options: MM+ Force Field with electrostatic contributions evaluated by atomic charges; all rotatable bonds on dodecamethylene (compound **3**) or the aromatic (compound **6**) chain were varied by the "torsional flexing" procedure of Kolossváry and Guida,[20] as implemented in the program; maximum number of retained conformers = 1000; acceptance energy criterion 3 kcal mol^{-1} above global minimum; maximum number of iterations and optimizations 100 000, 1000; maximum number of cycles 1000; rms gradient 0.01 kcal/(Å mol); conformations selected to vary chosen by usage directed; random number generation based on the computer's clock. Molecular dynamic simulations were performed in vacuum by molecular mechanics calculations (MM+ force field), with the electrostatic contributions evaluated by atomic charges. Other options were the following: heat time 0.5 ps, run time 3 ps, cool time 1 ps, step size 0.001 ps, starting temperature 0 K, simulation temperature variable from 323 to 423 K for **3** and from 323 to 675 K for **6**, final temperature 0 K, temperature step 30 K, constant temperature, and bath relaxation time 0.1 ps. Geometries of global minima (GM) coming from the conformational search on **3** and **6** were used as such within molecular dynamic simulations of the mechanism reported in Scheme 2, path A. Under the aforementioned conditions we did not observe enantiomerization for both **3** and **6** derivatives. GM of **3** and **6** were also modified by breaking the O···U coordinative bond on the side as the aromatic pendant and, after optimization in vacuum by the molecular mechanics method, the resulting geometries (GM^{U+O-}) were used as starting species to simulate the mechanism reported in path B. In both optimizations and dynamic simulations charges on oxygen and uranium atoms derived by the heterolytic O···U bond cleavage were set scaling their formally unitary values by a suitable factor to simulate the shielding effect of the solvents employed within the DHPLC determinations. The used factors, expressed as the reciprocal of the solvent permittivity, were 0.16 for **3** and 0.14 for **6** (permittivity values for the mixtures *n*-hexane/ethanol/$CHCl_3$ 50/30/20 and *n*-hexane/ethanol/methanol 60/30/10 were assessed according to the Kirkwood theory).[21] All molecular dynamic simulations on GM^{U+O-} of **3** led to an easy 360° rotation around the bond between the imine carbon atom and the disconnected phenoxide ring, independently from the set temperature. Instead, the same transformation was observed on GM^{U+O-} of **6** only at a temperature of 675 K. Analogous transformation was also recorded on GM^{U+O-} **6** at 363 K when charges on oxygen and uranium atoms were scaled by a factor 0.04, corresponding to a formal solvent permittivity of 25. In all cases of favorable rotation of the disconnected phenoxide ring, simulations of molecular dynamic

(20) Kolossváry, I.; Guida, W. C. *J. Comput. Chem.* **1993**, *14*, 691–698.
(21) Wang, P.; Anderko, A. *Fluid Phase Equilib.* **2001**, *186*, 103–122.

were completed by performing three other steps: (1) restoration of the O···U coordination bond within the GM^{U+O-} and subsequent optimization of the obtained structures to give the intermediates **I**; (2) rupture within the intermediates of the O···U bond placed on the same side as the methyl substituent on the second phenoxy moiety and subsequent optimization of the resulting structures $^{CH_3}GM^{U+O-}$; and (3) use of the $^{CH_3}GM^{U+O-}$ structures as starting geometries to perform new molecular dynamic simulations at the same conditions aforementioned. Always these simulations led to final geometries corresponding, after restoration of the O···U coordination bond and simple optimization, to the enantiomeric forms of the starting GM structures.

Summary and Conclusions

The chiral uranyl−salophen complex **3** featuring a dodecamethylene chain was expected by design to be configurationally stable. It was found, however, that **3** undergoes enantiomerization at high temperature, as revealed by DHPLC on an enantioselective column. A dissociation−reassociation mechanism of enantiomerization was immediately ruled out, because it would imply loss of material and release of the pure ligand in the HPLC runs. A simple jump rope mechanism was also excluded on the basis of a comparison with the dynamic behaviors of the structurally modified analogous derivatives **4** and **5**. The close similarity of the enantiomerization rate of **3** to those of **4** and **5** shows that it is independent of the extension of the salophen ligand. This is strongly suggestive of an enantiomerization mechanism based on ligand hemilability, heretofore unknown for metal complexes of sal(oph)en ligands. The dynamic behavior of complex **6**, featuring a more rigid bridge, fulfilled the expectations of a greater configurational stability. Compound **6**, whose half-life at room temperature was estimated to be a couple of months, turns out to be configurationally stable enough for use as a chiral receptor in enantioselective recognition and catalysis.

Acknowledgment. The work was supported by the Ministero dell'Università e della Ricerca (MUR) COFIN 2006 and PRIN, contract no. 2005037725.

Supporting Information Available: HPLC resolution and temperature-dependent chromatograms of **4** and **5**, calculated structure of the intermediate **I** for the enantiomerization of **3**, ^{1}H NMR spectra of **3** and **5** in the absence and presence of Pirkle alcohol, ^{1}H NMR spectra of all compounds, and ^{13}C NMR spectra of new compounds. This material is available free of charge via the Internet at http://pubs.acs.org.

JO800610F